Coordination and biological behaviour of 2-(*p*-toluidino)-N'-(3-oxo-1,3-diphenylpropylidene) acetohydrazide and its metal complexes

Ahmed N. Al-Hakimi[a]*, Abdou S. El-Tabl[b] and Mohamad M. E. Shakdofa[c]

[a]*Department of Chemistry, Faculty of Science, Ibb University, Ibb, Yemen*

[b]*Department of Chemistry, Faculty of Science, El-Menoufia University, Shebin El-Kom, Egypt*

[c]*Inorganic Chemistry Department, National Research Centre, P.O. 12622 Dokki, Cairo, Egypt*

A series of Ni(II), Co(II), Cu(II), Mn(II), Zn(II), Zr(IV), Fe(III), Ru(III), La(III), Hf(IV) and U(VI) complexes of 2-(*p*-toluidino)-N'-(3-oxo-1,3-diphenylpropylidene) acetohydrazide (H_2L) have been synthesised and characterised by elemental and thermal analyses (DTA, TG), molar conductances, magnetic moments, IR, ^{1}H NMR, UV-Vis spectra and ESR measurements. The ESR spectra of solid complexes $[(L)(HL)Cu_2(OAc)]$, $[Cu(HL)(H_2L)(NO_3)]$ and $[CuCl(HL)(H_2L)].H_2O$ at room temperature show axial symmetry with covalent bond character, and complex $[FeCl_2(HL)(H_2O)]$ has $g_{av} = 4.38$, indicating a high spin (5/2) iron(III) complex. However, complexes $[(HL)Mn_2Cl_3(H_2O)_4]$ and $[RuCl_2(HL)(H_2O)].H_2O$ have isotropic spectra consistent with octahedral structure. The antifungal and antibacterial activities of the ligand and its complexes were investigated.

Keywords: metal complexes, synthesis, spectra, thermal studies, magnetism, biological studies

There has been considerable recent interest in the synthesis of hydrazones and their complexes. Interest in these species stems largely from their applications as insecticides, in medicine and in analytical chemistry. 2,6-di-tert-butyl-4-(2-azinylhydrazonomethyl) phenol derivatives possess potential as 5-lipoxygenase inhibitors.[1] Metal complexes of hydrazones act as potential inhibitors for many enzymes.[2] The presence of heterocyclic rings in the synthesised hydrazones are responsible for pharmacological properties.[3] Hydrazones create environments similar to biological systems by coordination through oxygen and nitrogen atoms. These ligands coordinate with metal ions to produce stable metal complexes owing to their facile keto–enol tautomerism. Their complexes have been proposed as acid–base indicators,[4] reservoir sensors[5] and as analytical reagents[6] due to the colour intensification which accompanies deprotonation. Isonicotinoylhydrazone was found to be analogous to anti-tuberculosis drugs.[7] Also hydrazones are used as plasticisers and stabilisers for polymers,[8,9] polymerisation initiators and antioxidants.[10] Due to the above applications, we now report the syntheses and spectroscopic studies of 2-(*p*-toluidino)-N'-(3-oxo-1,3-diphenylpropylidene) acetohydrazide and its metal complexes.

Experimental

Reagent grade chemicals were used. 2-(*p*-toluidino) acetohydrazide was prepared by a published method.[11] Elemental analyses were determined by the Analytical Unit of Cairo University of Egypt. Standard analytical methods were used to determine the metal ion content.[20] All metal complexes were dried in vacuum over anhydrous $CaCl_2$. The IR spectra were measured using a Perkin-Elmer 683 spectrophotometer (4000–200 cm^{-1}). Electronic spectra in DMF solutions were recorded on a Perkin-Elmer 550 spectrophotometer. The conductances of the complexes (10^{-3} M DMF) were measured at 25 °C with a Bibby conductometer type MCl. The ^{1}H NMR spectrum of the ligand in DMSO-d_6 was recorded using a 300 MHZ Varian NMR spectrometer. The thermal analyses (DTA and TG) were carried out in air on a Shimadzu DT-30 thermal analyser from 27 to 800 °C at a heating rate of 10 °C per minute. Magnetic moments were measured using the Gouy method, $\mu_{eff.} = 2.84\sqrt{\chi_M^{corr}.T}$. ESR measurements of solid complexes at room temperature were made using a Varian E-109 spectrophotometer, with DPPH as a standard material. TLC was used to confirm the purity of the compounds.

Preparation of the ligand **(1)** *[H_2L]*

2-(*p*-toluidino) acetohydrazide (1.7 g, 0.01 mol) was dissolved in EtOH (25 mL) and dibenzoylmethane (2.3 g, 0.01 mol) dissolved in EtOH (15 mL) was added dropwise. The reaction mixture was refluxed for 3 h, then cooled to room temperature and the product was filtered off, washed several times with EtOH and dried over anhydrous $CaCl_2$.

Preparation of metal complexes **(2)–(20)**

Metal complexes were prepared by mixing stiochiometric ratios (L:M) (1:1 or 2:1) of the ligand (H_2L) in EtOH (30 mL) with the appropriate metal salts (in 50 mL EtOH/15 mL H_2O). The mixture was refluxed for 2–3 h. On cooling to room temperature, fine crystals formed, which were filtered off, washed with EtOH and dried over anhydrous $CaCl_2$.

In-vitro *antibacterial and antifungal activities*

The antibacterial and antifungal activities of the ligand and its metal complexes have been studied by the disc diffusion method.[13,14] using the organisms *Escherichia coli, Bacillus subtilis* and *Aspergillus niger*. The test compounds were dissolved in DMSO to concentrations of 250, 200, 175, 150 and 125 ppm and a DMSO poured disc was used as negative control. The bacteria were subcultured in nutrient agar medium, which was prepared using peptone, beef extract, NaCl, agar agar and distilled water. The Petri dishes were incubated for 48 h at 37 °C. The standard antibacterial drug tetracycline was also screened under similar conditions for comparison. The fungi were subcultured in Dox´s medium, which was prepared using yeast extract, sucrose, $NaNO_3$, agar agar, KCl, KH_2PO_4, $MgSO_4.7H_2O$, distilled water and trace of $FeCl_3.6H_2O$. The standard antifungal drug amphotricene B was also used for comparison. The Petri dishes were incubated for 48 h at 28 °C.The zone of inhibition was measured in millimetres carefully. All determination was made in duplicate for each of the compounds. An average of the two independent readings for each compound was recorded.

Results and discussion

Reaction of 2-(*p*-toluidino)acetohydrazide with dibenzoylmethane in EtOH 1:1, molar ratio, led to the formation of 2-(*p*-toluidino)-N'-(3-oxo-1,3-diphenylpropylidene) acetohydrazide (H_2L) (Fig. 1). The reaction of the ligand (H_2L), with the metal salts using (1:1) or (2:1) molar ratios, gave intensely coloured, crystalline solids, which are stable at room temperature and do not decompose after prolonged storage. The complexes are insoluble in water, ethanol, methanol, benzene, toluene, acetonitrile and chloroform, but completely soluble in dimethylformamide (DMF) or dimethylsulfoxide (DMSO). Elemental analyses and physical data (Table 1), and spectral data [Tables 2 and 3, deposited in the Electronic Supplementary Information (ESI)], are compatible with the proposed structures (Fig. 2). To date, no diffractable crystals could be obtained.

^{1}H NMR spectrum

The ^{1}H NMR spectrum of the ligand in DMSO-d_6 shows signals which are consistent with the proposed structure (ketonic form, Fig. 1). The observed peaks at 9.8 and 8.89 ppm are assignable to the protons of the NH groups of the hydrazide and amine moieties respectively[2] confirming that the ligand is present in the ketonic

* Correspondent. E-mail: anmalhakimi@yahoo.com

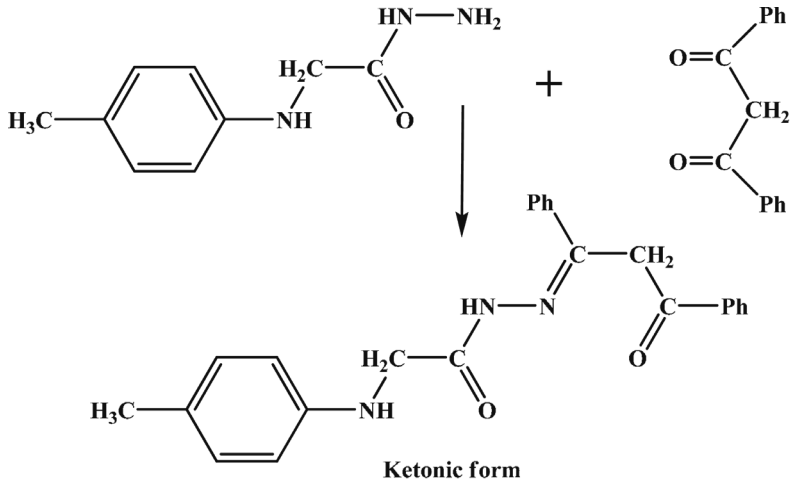

(2-(*p*-toluidino)-*N*'-(3-oxo-1,3-diphenylpropylidene)acetohydrazide

Fig. 1 Preparation of the ligand.

Table 1 Elemental analyses and physical properties of the ligand and its metal complexes

No.	Compounds	Colour	M.p.	Yield	Ω mol^{-1}	Found (Calcd)/%				
			/C°)	/%	cm^2	C	H	N	Cl	M
1	$[H_2L]$ ($C_{24}H_{23}N_3O_2$)	Yellow	60	80	----	74.4(74.5)	5.97(6.2)	10.9(10.6)	–	–
2	$[(HL)(H_2L)Ni(OAc)(H_2O)].3H_2O$	Red	240	79	3.3	63.8(63.8)	5.5(5.7)	8.76 (9.0)	–	6.5(6.2)
3	$[(L)(HL)Ni_2(NO_3)]$	Green	180	75	3.8	61.0(60.7)	4.2(4.5)	10.5(10.3)	–	12. 6(12.4)
4	$[(L)(HL)\ Ni_2Cl].3H_2O$	Yellow	215	76	4.8	59.0(59.0)	4.9(5.1)	8.8(8.6)	4.0(3.4)	12.3(12.0)
5	$[(L)Co_2(OAc)_2(H_2O)].3H_2O$	Brown	250	78	5.2	48.6(48.6)	4.9(5.1)	6.0(6.1)	–	17.0(17.1)
6	$[(H_2L)Co_2(NO_3)_4(H_2O)_3].H_2O$	Brown	240	75	4.3	35.0(35.0)	4.6(3.8)	12.1(11.9)	–	12.6(14.3)
7	$[(L)(HL)Co_2Cl].2H_2O$	Brown	170	78	3.8	60.1(60.2)	5.4(4.9)	9.2(8.8)	4.0 (3.7)	12.1(12.3)
8	$[(L)(HL)Cu_2(OAc)]$	Brown	240	82	4.1	63.063.0)	4.7(4.8)	8.8(8.8)	–	13.8(13.3)
9	$[(HL)(H_2L)Cu(NO_3)\ (H_2O)]$	Brown	255	80	3.5	64.4(64.4)	4.9(5.0)	11.0(11.0)	–	7.8(7.1)
10	$[(HL)(H_2L)CuCl(H_2O)].H_2O$	Green	180	79	2.8	65.1(65.1)	4.6(5.2)	9.1(9.5)	4.5(4.0)	7.5(7.2)
11	$[(HL)Mn_2Cl_3(H_2O)_4]$	Yellow	170	71	4.8	42.7(42.8)	4.5(4.4)	6.2(6.2)	15.5(15.8)	16.8(16.3)
12	$[(HL)FeCl_2(H_2O)]$	Brown	200	72	6.5	51.1(51.0)	4.4(4.4)	7.7(7.4)	18.4(18.8)	9.7(9.9)
13	$[(HL)RuCl_2(H_2O)].H_2O$	Black	105	78	7.3	49.1(48.6)	4.6(4.4)	7.5(7.1)	11.5(12.0)	16.8(17.1)
14	$[(HL)ZrOCl].3H_2O$	Green	230	83	7.8	49.5(49.6)	4.8(4.8)	7.0(7.3)	6.4(6.1)	15.7 (15.7)
15	$[(HL)_2HfCl_2\ ].4H_2O$	Green	220	81	8.2	52.1(52.9)	4.6(4.8)	7.3(7.7)	6.8 (6.5)	15.8(16.4)
16	$[(HL)Zn(OAc)]$	Yellow	140	85	5.2	62.0(61.3)	5.0(4.9)	8.5(8.2)	–	12.81(12.8)
17	$[(HL)Zn(NO_3)]$	Green	220	82	6.2	57.0(56.3)	4.7(4.3)	10.7(11.0)	–	13(12.8)
18	$[(HL)ZnCl].3H_2O$	Orange	200	80	5.5	54.0(53.5)	4.6(5.2)	8.2(7.8)	6.9 (6.6)	12.2(12.1)
19	$[(HL)LaCl_2(H_2O)]$	Orange	300	84	5.4	47.2(47.1)	3.8(3.9)	6.7(6.9)	5.7(5.8)	23.1(22.7)
20	$[(HL)(UO_2)(OAc)\ ].2H_2O$	Yellow	175	85	6.5	41.9(41.7)	3.7(3.9)	5.6(5.6)	–	31.5(31.8)

form with no evidence for the presence of the enol form from the appearance of the NH signal and also the absence of the signal OH of the enol form. Multiplet signals in the 7.73–6.8 ppm range are due to aromatic protons.[11] The resonances at 5.17, 4.9 and 2.40 ppm correspond to the protons of methylene groups of the acetohydrazide and dibenzoyl moieties and methyl groups respectively.[15,16]

Conductivity measurements

The molar conductance values of the complexes are in the (2.8–8.2 $\Omega^{-1}cm^2mol^{-1}$) range (Table 1), these low values indicate the non–electrolytic nature of the complexes.[15] This confirms that the anion is coordinated to the metal ion.

IR spectra

Important spectral bands of the ligand and its complexes are presented in Table 2 (deposited in the ESI). The IR spectrum of the ligand (H_2L) shows broad, medium intensity bands in the 3650–3260 and 3245–2780 cm^{-1} ranges, which are attributed to intra- and inter-molecular hydrogen bonding.[17] The spectrum shows bands at 3405, 3270, 1714 and 1656 cm^{-1}, assigned to the ν(NH), ν(C=O) and ν(C=N) respectively,[18,19] confirmed the ketonic form of the ligand. Also, a band appears at 1597 cm^{-1} corresponding to $\nu(C=C)_{Ar}$.[19,20] In order to know the mode of coordination between the ligand and the metal ion, the IR spectrum of the ligand was compared with those of the metal complexes. The complexes show broad bands in the 3565–3225 and 3260–2730 cm^{-1} ranges due to intra- and intermolecular hydrogen bondings[17] and other bands in the 3350–3100 and 827–755 cm^{-1} ranges are due to the presence of coordinated water molecules as in complexes **(5), (6), (11), (12), (13)** and **(19)**, whereas the band which appears in the 3670–3340 range is due to the presence of water molecules of hydration as in complexes **(2), (4–7), (10), (13–15), (18)** and **(20)**.[17,20,21] However, ν(NH) appears in the 3435–3348 and 3255–3200 cm^{-1} ranges[20,21] (Table 2, deposited in the ESI). The complexes show a band in the 1711–1640 cm^{-1} range (Table 2, deposited in the ESI), which is assigned to ν(C=O) except for complex **(5)**.[22] The bands that appear in the 1650–1594, 1596–1549, 1543–1517 and 1389–1223 cm^{-1} ranges are due to ν(C=N), $\nu(C=C)_{Ar}$ and ν(CH=C) and ν(C-O) vibrations respectively.[19,20,23] For metal acetate complexes the monodentate coordination is shown by the occurrence of $\nu_a(CO_2)$ at a frequency lower than $\nu_s(CO_2)$,[24,25] As a result, the separation between the two bands is much larger in monodentate complexes as in complexes **(2), (5), (16)** and **(20)** (*i.e.*, $\nu_a(CO_2)$ = 1556, 1605, 1540 and 1605 cm^{-1}, $\nu_s(CO_2)$ = 1417, 1398, 1417 and 1400 cm^{-1} respectively). In addition, complex **(5)** shows $\nu(CO_2)$ at 1549 and 1456 cm^{-1} due to a bridging acetate group.[24,25] Complexes **(3), (6), (9)** and **(17)** show several bands in the 1398–1383, 1229–1181 and 850–835 cm^{-1} ranges (Table 2, deposited in the ESI), assigned to a bridging or coordinating nitrate group.[25,26] Complexes **(4), (7), (8), (10–15), (18)** and **(19)** show bands in the 423–419, 370–350 cm^{-1} ranges corresponding to coordinated and bridging chloride atoms. However, complex **(14)** shows a band at 760 cm^{-1} assigned to ν(ZrO).[27] Complex **(21)** shows a band at 940 cm^{-1} due to its O = U = O group.[27]

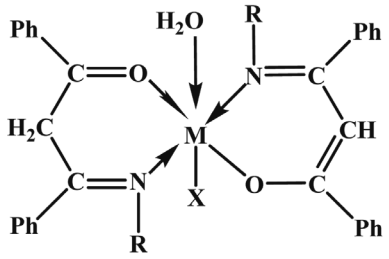

$[(HL)(H_2L)MX(H_2O)].nH_2O$
M= Ni(II), X= OAc, n= 3 (2)
M= Cu(II), X= NO_3, n= 0 (9)
M= Cu(II), X= Cl, n= 1 (10)

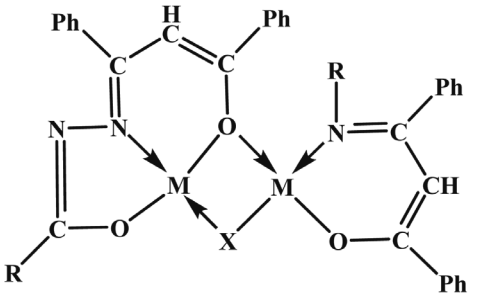

$[(HL)(L)M_2X].nH_2O$
M= Ni(II), X= NO_3, n= 0 (3)
M= Ni(II), X= Cl, n= 3 (4)
M= Co(II), X= Cl, n= 2 (7)
M= Cu(II), X= Cl, n= 0 (8)

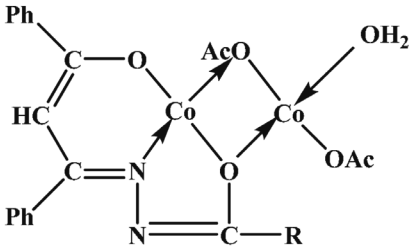

$[(L)Co_2(OAc)_2(H_2O)].3H_2O$
(5)

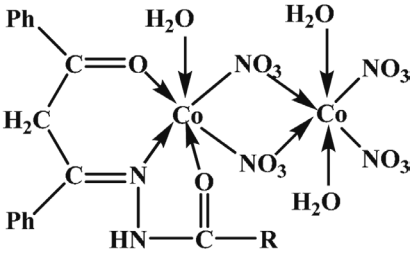

$[(H_2L)Co_2(NO_3)_4(H_2O)_3].H_2O$
(6)

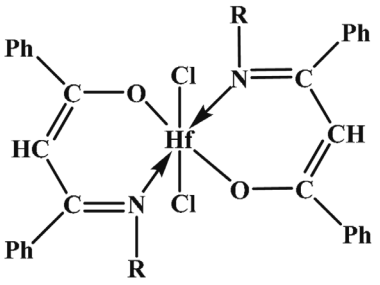

$[(HL)_2HfCl_2].4H_2O$
(15)

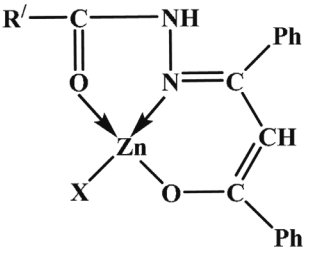

$[(HL)ZnX].nH_2O$
X= OAc, n= 0 (16)
X= NO_3, n= 0 (17)
X= Cl, n= 3 (18)

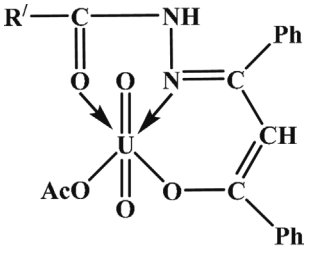

$[(HL)UO_2(OAc)].2H_2O$
(20)

$R^{/}$= $CH_3C_6H_4NHCH_2$ -
R=$R^{/}CONH$

Fig. 2 Structural representation of metal complexes.

The spectral results together with elemental analyses indicated that the hydrazone can behave as a neutral bidentate (H_2L), monobasic bidentate (HL^-), monobasic tridentate (HL^-) or dibasic tridentate (L^{2-}) ligand towards the metal ions, and also, the ligand is coordinated to the metal ion by the carbonyl oxygen of the hydrazide moiety and carbonyl oxygen of the dibenzoylmethane moiety in the enolic or ketonic form, as well as by azomethine nitrogen atoms.

Magnetic moments

Room temperature magnetic moments of the complexes **(2–20)** are shown in Table 3 (deposited in the ESI). Nickel(II) complexes **(3)** and **(4)** show diamagnetic values confirming a square planar geometry around the nickel(II) ion. However, complex **(2)** shows 2.74 B.M., indicating octahedral geometry around the nickel(II) ion.[24,28] Cobalt(II) complexes **(5), (6)** and **(7)** show values 3.4 and 4.2 and 3.2 B.M. (Table 1), which could indicate high spin square planar or octahedral cobalt(II) complexes.[8,29] However, the low values of **(5)** and **(7)** indicate spin-exchange interactions take place between the cobalt(II) ions in a square planner geometry. The magnetic moments for the copper(II) complexes **(8), (9)** and **(10)** are 1.5, 1.81 and 1.72 B.M respectively**.** The value of complex **(8)** is well below the spin-only value (1.73 B.M.), indicating spin-exchange interactions take place between the copper(II) ions in a square planar environmental.[30] However, the values of complexes **(9)** and **(10)** correspond to one unpaired electron in an octahedral structure.[8] The magnetic moment value for manganese(II) complex **(11)** is 4.92 B.M., suggesting a high spin octahedral geometry around the manganese(II) ion.[17] The low value is due to the presence of spin-exchange interactions between the Mn(II) ions. Iron(III) complex **(12)** shows a value 5.66 B.M, indicating a high spin iron(III) octahedral geometry.[8] Ruthenium(III) complex **(13)** shows a magnetic value 1.6 B.M indicating an octahedral structure.[31] Zirconium(IV) **(14),** hafnium(IV) **(15),** zinc(II) complexes **(16–18),** lanthanum(III) **(19)** and uranyl(II) **(20)** complexes are diamagnetic.

Electronic spectra

The electronic spectral data of the ligand and its complexes in DMF solution are presented in Table 3 (deposited in the ESI). The ligand exhibits bands at 310 and 220 nm, assigned to n→π* and π→π*transitions.[17] The nickel(II) complex **(2)** shows bands at 345, 480 and 650 nm; the bands are attributable to $^3A_{2g}(F)\rightarrow{}^3T_{1g}(P)$ (υ_3), $^3A_{2g}(F)\rightarrow{}^3T_{1g}(F)$ (υ_2) and $^3A_{2g}(F)\rightarrow{}^3T_{2g}(F)$ (υ_1) transitions respectively of an octahedral nickel(II) complex.[32] The υ_2/υ_1 ratio is 1.37 indicating a distorted octahedral nickel(II) complex.[33] However, complexes **(3)** and **(4),** show bands at 460 and 510 and 450 and 520 nm respectively. The bands are assigned to $^3T_1\rightarrow{}^3T_2$ and $^3T_1(F)\rightarrow{}^3T_2(P)$ transitions, of a square planar nickel(II) ion.[27,34] The cobalt(II) complexes **(5)** and **(7)** show bands in the 460, 545 and 620 nm and 475, 555 and 610 nm respectively are which assigned to a square planar geometry.[35] However, complex **(6)** shows bands at 455, 550 and 650 nm; these bands are assigned to $^4T_{1g}(F)\rightarrow{}^4T_{2g}(F)$, $^4T_{1g}(F)\rightarrow{}^4A_{2g}$ and $^4T_{1g}(F)\rightarrow{}^4T_{1g}(P)$ transitions respectively of a high spin cobalt(II) octahedral complex.[36] The copper(II) complexes **(8), (9)** and **(10)** show different bands (Table 3, deposited in the ESI). Complex **(8)** shows bands at 395, 480 and 590 nm, corresponding to $^2B_{1g}\rightarrow{}^2B_{2g}$, $^2B_{1g}\rightarrow{}^2E_g$ and $^2B_{1g}\rightarrow{}^2A_{1g}$ transitions respectively of a square planar geometry.[37] However, complexes **(9)** and **(10)** show bands at 390, 475 and 640 nm and 395, 480, 650 nm respectively. The bands are assigned to ligand→copper charge transfer, $^2B_1\rightarrow{}^2E$ and $^2B_1\rightarrow{}^2B_2$ transitions, in a distorted octahedral structure.[38] Manganese(II) complex **(11)** shows bands at 485, 550 and 650 nm, corresponding to $^6A_{1g}\rightarrow{}^4E_g$, $^6A_{1g}\rightarrow{}^4T_{2g}$ and $^6A_{1g}\rightarrow{}^4T_{1g}$ transitions which are compatible to an octahedral geometry around the manganese(II) ion.[39] Iron(III) complex **(12)** shows bands at 475, 550 and 640 nm. The first two bands are due to charge transfer transitions while the last band is considered to arise from the $^6A_1\rightarrow{}^4T_1$ transition; these bands suggest a distorted octahedral geometry around the iron(III).[35,37] Ruthenium(III) complex **(13)**, shows bands at 475, 575 and 620 nm. The first bands are due to LMCT transitions and the other band is assigned to a $^2T_{2g}\rightarrow{}^2A_{2g}$ transition. The band positions are similar to those observed for other octahedral ruthenium(III) complexes.[31,40] Zirconium(IV) complex **(14)**, hafnium(IV) **(15),** zinc(II) **(16-18),** lanthanum(III) **(19)** and uranyl(VI) **(20)** complexes show bands (Table 3, deposited in the ESI) indicating intraligand transitions.[37,41]

Electron spin resonance

The ESR spectra of solid copper(II) complexes **(8)**, **(9)** and **(10)** at room temperature are characteristic of a specie with a d^9 configuration and having an axial symmetry type of a $d_{(x2-y2)}$ ground state, which is the most common for copper(II) complexes.[33,42] The g-values suggest a square planar or octahedral geometry[23] and the complexes show $g_\parallel > g_\perp > 2.0023$, indicating a distortion around the copper(II) ion[43,44] The ESR parameters for the complexes are shown in Table 4 (deposited in the ESI). The g-values are related by the expression,[43,44] $G = (g_\parallel - 2)/(g_\perp - 2)$. If $G > 4.0$, then local tetragonal axes are aligand parallel or only slightly misaligand and if $G < 4.0$, significant exchange coupling is present. Complex **(8)** shows a value of 3.33, indicating spin-exchange interaction takes place between copper(II) ions, which is compatible with the magnetic moment value. However, complexes **(9)** and **(10)** show $G > 4.0$ (Table 4, deposited in the ESI), indicating tetragonal axes are present in these complexes. Also, the $g_\parallel/A_\parallel$ values are considered as diagnostic of stereochemistry.[43,44] The $g_\parallel/A_\parallel$ value for the complexes (Table 6, deposited in the ESI) lie just within the range of expected structures. The $g_|$ -values reported here are 2.2, 2.26 and 2.27 respectively, indicating considerable covalent bonding character in these complexes.[23,42,43] The isotropic value of the hyperfine coupling constant A_{iso} is related to the σ-bonding parameter (α^2).[44,46] If $\alpha^2 = 1$, the bond would be completely ionic and if $\alpha^2 = 0.5$, the bond would be completely covalent. The calculated values of α^2 for complexes **(8), (9)** and **(10)** are 0.73, 0.64 and 0.63 respectively, suggesting covalent bonding.[42,44] The orbital reduction factor (K)[45] can be used to measure the covalent character of the metal-ligand band. For an ionic environmental, $K = 1$ and for a covalent environmental $K < 1$; the lower the value of K, the greater is the covalent character. The K-values for the complexes (Table 4, deposited in the ESI) are indicative of a covalent nature.[23,42,43] Also, the in-plane and out-of plane π-bonding coefficients (β_1^2 and B^2) can be calculated.[23,42,43] The complexes show β^2 and β^2_1 values (Table 6, deposited in the ESI) that indicate ionic character in the in-plane π and covalent character in out-of plane π-bonding.[46] It is possible to calculate approximate orbital populations for p or d orbitals using the following equations,[47] where A^o and $2B^0$ are the calculated dipolar couplings for unit occupancy of s and d orbitals respectively.

$$A_{11} = A_{iso} - 2B[1 \pm (7/4)\,\Delta g_{11}] \quad (1)$$

$$\alpha^2_{p,\,d} = 2B/2B^0 \quad (2)$$

When the data are analysed using the Cu^{63} hyperfine coupling and considering all the sign combinations, for complexes **(8)**, **(9)** and **(10)** the only physically meaningful results are found when A_{11} and $A_\perp$ are negative. The resulting isotropic coupling constant and the parallel component of the dipolar coupling) are negative. The orbital population (α_d^2 %) for the complexes (Table 4, deposited in the ESI) indicate that the main orbital is the $d_{(x2-y2)}$ ground state.[44] However, the ESR spectra of manganese(II) and ruthenium(III) complexes are of the isotropic type with $g_{iso} = 2.024$ and 2.11 respectively, typical of octahedral structure. The iron(III) complex **(12)** shows $g_{av} = 4.38$ arising from very large zero field splitting effect. This g- value indicates a high spin (5/2) octahedral geometry around the iron(III) ion.

Thermal analyses

The results of TG and DTA analyses of complexes are shown in Table 5 (deposited in the ESI). The results show that complexes **(2)**, **(4)**, **(13–15)** and **(18)** lose hydrated water molecules in the temperature range 60–100 °C; this process is accompanied by an endothermic peak. The coordinated water molecules were eliminated from complexes **(2), (6), (11)** and **(13)** at relatively higher temperature than those of the hydrated water molecules (110–170 °C) (Table 5, deposited in the ESI). The removal of an HCl molecule (accompanied by an endothermic peak) was observed for **(4)**, **(11)**, **(13–15)** and **(18)** complexes in the temperature 240–310 °C range, compatible with the TG result. For complex **(6),** the removal of an HNO_3 molecule, also accompanied by an endothermic peak, was observed in the 280–295 °C range, compatible with the TG result. The removal of a CH_3COOH molecule, (accompanied by an endothermic peak), for complex **(12)** occurs at 320 °C, compatible with the TG result. The complexes decompose through degradation of the hydrazone ligand at a temperature above 400 °C leaving metal oxides (490–660 °C) (Table 5, deposited in the ESI).

Antibacterial and antifungal screening

The ligand and its complexes have been screened for their antibacterial and antifungal activities and the results obtained are presented in Table 6 (deposited in the ESI). It is observed that the activity of the complexes increases with increase in the concentration

of the compounds tested. All the metal complexes are more potent bactericides and fungicides than the ligand.[49-50] The results (Table 6, deposited in the ESI) show that Ru(III) complex **(13)** has higher antibacterial activity but Zn(II) complex **(18)** shows higher antifungal activity than the other complexes. For bacteria, the order of activities of these complexes is **(13)>(19)>(10) = (18)>(12)> (4)>(11)>(7)>(15)>(14) = (1)** and for fungi, the order of activities is **(18)>(10) = (13) = (19)>(11)>(12) = (14)>(4) = (15)>(7) = (1).** The variation in the activity of different complexes against different microorganisms depends either on the impermeability of the microbel cells or differences in the ribosomes of microbial cells. The increased activity of the metal chelates can be explained on the basis of chelation theory.[49] It is known that chelation tends to make the coordinated ligand act as more powerful and potent bacterial and fungicidal agent, thus killing more of the bacteria and fungi than the free ligand precursor. It is observed that in a complex, the positive charge of the metal is partially shared with the donor atoms present in the ligand and there may be π-electron delocalisation over the whole chelate.[51] This increases the lipophilic character of the metal chelate and favours its permeation through the lipoid layer of the organism membrane. There are other factors which also increase the activity, which are the number of coordination sites, size of complex, solubility, conductivity and also the bond lengths between the metal and the coordinated ligand atoms.

Received 2 September 2009; accepted 26 November 2009
Paper 09/0772 doi:10.3184/030823409X12596063380927
Published online: 8 December 2009

References

1 A. Cuadro, M.J. Valenciano, J. Vaquero, C. Alvarez-Builla, M. Sunkel, F. de Casa-Juana and M.P. Ortega, *Bioorg. Med. Chem*., 1998**, 6,** 173.
2 R. Gup and B. Kirkan, *Spectrochim. Acta,* Part A, 2005**, 62,** 1188.
3 S. Fucharion, R.T. Rowley and N.W. Paul (eds) *Thalassemia: pathophysiology and management,* Part B, R. Alan Liss, New York, 1988.
4 A.J. Cameron and N.A. Gibson, *Anal. Chim. Acta,* 1970**, 249,** 257.
5 R. Montes and J. Laserna, *J. Anal. Sci.,* 1991, 467.
6 R.B. Singh, P. Jain and R.P. Singh, *Talanta,* 1982, **29,** 77**.**
7 N. Georgevia and V. Gadjeva, *Biochemistry* (Moscow), 2002, **67,** 588.
8 Q. Albert, Nature 1953, **9,** 370, U. Kuehn, S. Warzeska, H. Pritzkow and R. Kraemer, *J. Am. Chem. Soc*., 2001, **123,** 6125.
9 J.M. Price, Fed. Proc. 1961, **20,** 223, K.D. Karlin and J. Zubieta *Copper coordination chemistry: biochemistry chemical and inorganic perspectives*, Adenine Press Guilderland, New York, 1983.
10 A.G. Mauk, R.A. Scott and H.B. Gray, *J. Am. Chem. Soc*., 1980**, 102**, 4360.
11 A.S. El-Tabl, F.A. El-Saied and A.N. Al-Hakimi, *Trans. Met. Chem*., 2007**, 32**, 689.
12 G. Svehla *Vogel's textbook of macro and semimicro quantitative inorganic analysis*, 5th edn, Longman Inc. New York 1979, pp. 212, 241, 259, 265, 272.
13 E.O. Offiong and S. Martelli, *Farm. I.L.*1994**, 49**, 513.
14 J.G. Collee, J.P. Duguid, A.G. Farser and B.D. Marmion (eds), *Practical medical microbiology*, New York, Churchill Livingstone, 1989.
15 K.B. Gudasi, S.A. Patil, R.S. Vadvavi, R.V. Shenoy and M. Nethaji, *Trans. Met. Chem*., 2006**, 31,** 586.
16 K.B. Gudasi, M.S. Patel, R.S. Rashmi, V. Shenoy, S.A. Patil and M. Nethaji, *Trans. Met. Chem*., 2006**, 31,** 580.
17 A.S. El-Tabl, F.A. El-Saied, W. Plass and A.N. Al-Hakimi, *Specteochim. Acta,* 2008, **71,** 90.
18 A.S. El-Tabl, T.I. Kasher, R.M. El-Bahnaswy and A.E. Ibrahim, *Pol. J. Chem*., 1999**, 73,** 245.
19 H.A. El-Boraey and A.S. El-Tabl, *Pol. J. Chem*., 2003**, 77,** 1759.
20 A.S. El-Tabl, K. El-Baradie and R.M. Issa, *J. Coord. Chem*., 2003**, 56,** 1113.
21 W.H. Hegazy, *Monat. Chem*., 2001**, 132**, 639.
22 A.S. El-Tabl, F.A. El-Saied and A.N. Al-Hakimi, *J. Coord. Chem*., 2008**, 61,** 2380.
23 A.S. El-Tabl, *Trans. Met. Chem*., 2002, **27,** 166.
24 A.S. El-Tabl, *J. Chem. Res. (S),* 2002, 529.
25 K. Nakatamato *Infrared spectra of inorganic and coordination compounds*, 2nd edn, Wiley Inc. New York, 1967.
26 H.M. El-Tabl, F.A. El-Said and M.I. Ayad, *Synth. React. Inorg. Met.-Org. Nano-Met. Chem*., 2005, **35,** 243.
27 R.A. Lal and A. Kumar, *Ind. J. Chem*., 1999**, 38A,** 839.
28 J.K. Nag, S. Pal and C. Sinha, *Trans. Met. Chem*., 2005**, 30**, 523.
29 N. Raman, Y. Pitchaikani and A. Kulandaisamy, *Proc. Indian Acad. Sc. (Chem. Sc.),* 2001**, 133,** 183.
30 A. El-Motaleb, M. Ramadan, W. Sawodny, H.F. El-Baradie and M. Gaber, *Trans. Met. Chem.,* 1997**, 22,** 211.
31 A.S. El-Tabl and M.I. Ayad, *Synth. React. Inorg. Met.-Org. Chem*., 2003**, 33,** 369.
32 D.N. Sathyanarayana, *Electronic absorption spectroscopy and related techniques*, Orient Longman Limited © Universities press (India) Limited (2001).
33 A.S. El-Tabl and S.A. El-Enein, *J. Coord. Chem*., 2004**, 57,** 281.
34 A. Cukurovali, I. Yalmaz and S. Kirbag, *Trans. Met. Chem*., 2006**, 31,** 207.
35 S.M. Ben-Saber, A.A. Maihub, S.S. Huder and M.M. El-Ajaily, *Microchem. J.,* 2005, **81,** 191.
36 S. Chandra and U. Kumar, *Spectrochim. Acta, Part A,* 2005**, 61,** 219.
37 S.A. Sallam, A.S. Orabi, B.A. El-Shetary and A. Lentz, *Trans. Met. Chem*., 2002**, 27,** 447.
38 R K. Parihari, R.K. Patel and R.N. Patel, *J. Indian Chem. Soc*., 2000**, 77,** 339.
39 N.K. Singh and S.B. Singh, *Trans. Met. Chem*., 2001**, 26,** 487.
40 A.S. El-Tabl, R.M. Issa and M.A. Morsi, *Trans. Met. Chem*., 2004**, 29,** 543.
41 B.D. Wang, Z.Y. Yang, Q. Wang, T.K. Cai and P. Crewdson, *Bioorg. Med. Chem*., 2006**, 14,** 1880.
42 A.S. El-Tabl, *Bull. Korean Chem. Soc*., 2004**, 25,** 1.
43 A.S. El-Tabl, *Trans. Met. Chem.,* 1996**, 21,** 428.
44 A.S. El-Tabl, *Trans. Met. Chem*., 1998**, 23,** 63.
45 R.K. Ray, *Inorg. Chem. Acta*,1990**, 174,** 257.
46 Z.W. Mao, K.B. Yu, D. Chen, S.Y. Han, Y.X. Sui and W.X. Tang, *Inorg. Chem*.**,** 1993**, 32,** 2140.
47 M.C.R. Symons, *Chemical and biochemical aspects of electron spin resonance*, Van Nostrand Reinhold, Wokingham, 1979.
48 B.A. Goodman and J.B. Raynor, *Advances in inorg. Chem. Radiochem*., 1970**, 13,** 268.
49 D. Sriram, P. Yogeeswari and R.V. Devakaram, *Bioorg. Med. Chem*., 2006, **14,** 3113.
50 S.K. Sridhar, M. Saravanan and A. Ramsh, *Eur. J. Med. Chem*., 2001, **36,** 615.
51 S.K. Sengupta, O.P. Pandy, B.K. Srivastava and V.K. Sharma, *Trans. Met. Chem*., 1998, **23**, 349.